A COMPARATIVE STUDY OF CONVENTIONAL AND ADVANCED PI CONTROLLERS FOR INDUCTION MOTOR SPEED REGULATION UNDER PARAMETER VARIATIONS

Yesma BENDAHA*, Kadda BOUMEDIENE, Bachir DAAOU****

*Faculty of Electrical Engineering, Department of Automation, LDEE Laboratory ,University of Science and Technology Mohamed Boudiaf, El Mnaouar, BP1505, Bir El Djir, Oran, 31000, Algeria
**Faculty of Electrical Engineering, Department of Automation, University of Science and Technology Mohamed Boudiaf, El Mnaouar, BP1505, Bir El Djir, Oran, 31000, Algeria

yesma.bendaha@univ-usto.dz, kadda.boumediene@univ-usto.dz, bachir.daaou@univ-usto.dz

received 07 October 2025, revised 29 January 2026, accepted 30 January 2026

Abstract: This paper presents a comparative study of various Proportional-Integral (PI) controller strategies applied to the speed regulation of a squirrel-cage induction motor under Indirect Field-Oriented Control (IFOC). The classical PI controller is benchmarked against three enhanced versions: the Hyperbolic PI (HPI), the Variable Gain PI (VGPI), and the Anti-Windup PI. Each controller is evaluated in terms of dynamic response, steady-state error, robustness to parameter variations and disturbance rejection. In addition, various numerical simulations under MATLAB/Simulink are carried out to evaluate the motor's performance through different operating conditions, including load disturbances and reference speed changes. The obtained numerical results conclude that, among the modified PI variants, the VGPI and Anti-Windup PI demonstrate superior performance in terms of robustness, adaptability, and transient behaviour. The obtained numerical results highlight the advantages and limitations of the control strategy, providing valuable insights for selecting an appropriate speed regulator in industrial applications.

Key words: field oriented control, conventional and advanced PI, induction motor speed regulation, parameters variations

1. INTRODUCTION

Induction Motors (IMs) are widely used in industrial applications due to their robustness, low maintenance requirements and cost-effectiveness. However, controlling high precision speed remains a challenging task especially under varying load conditions and parameter uncertainties [1-2]. To overcome these challenges, Indirect Field-Oriented Control (IFOC) has been widely adopted as it allows decoupled control of flux and torque making the behave motor induction similar to a separate DC motor excited [3-4].

The core control speed loop in an IFOC scheme lies the Proportional-Integral controller that is traditionally favoured for its simplicity and effectiveness to maintain a desired speed [5]. However, the conventional PI controller often suffers from limitations such as poor performance in transient conditions, sensitivity to tuning parameters and integrator windup during large disturbances or saturation [6-8].

To debate these issues, several modified PI controllers have been proposed including the Hyperbolic PI [9], Variable Gain PI [10], and Anti-Windup PI regulators [11-12]. Each strategy introduces specific enhancements to improve dynamic response, robustness, and overall system performance. The HPI utilizes nonlinear hyperbolic functions to enhance gain response, VGPI adapts controller gains in real-time based on system error or dynamics, while the Anti-Windup PI evaluates integrator saturation problems.

In the last few years, several technics for controlling the speed regulation of induction motors have been developed. In reference [13], Soukaina El Daoudi et al. presents an improved direct torque control strategy for induction motors, utilizing a five-level diode-clamped inverter and a sensor-less algorithm. The study reduces torque and flux ripples, and the authors validate their method's efficiency by comparing it with other inverter topologies. Authors in [14] present two modified strategies for Direct Torque Control (DTC) of asynchronous motors, focusing on improving performance and reducing ripples. It introduces a sliding mode control approach combined with sinusoidal pulse width modulation, aiming to enhance dynamics and reliability without the use of mechanical sensors. Najib El Ouanjli et al. [15] present an improved Direct Torque Control (DTC) strategy for induction motors, utilising a twelve-sector approach combined with a back-stepping speed controller and a robust model reference adaptive system for stator resistance estimation. The proposed methods enhance motor performance and stability, validated through simulations and experiments using a dSPACE DS1104 board.

Emre Çelik et al. [16] used a non-linear PI controller in order to improve velocity regulation in PMDC motor drive. The obtained numerical results are in good accordance with other results in the literatures, the proposed non-linear PI (EXP-PI) controller achieved a good performance. Nichat Orturk and Emre Çelik [17] proposed a new alternative method based on SOS algorithm (Symbiotic Organisms Search) to improve a Direct Current (DC) motor drive's dynamics and performance; the obtained numerical results demonstrate that the proposed algorithm gives an important optimization for effective PI controller design. A cascade one proportional derivative incorporating filter (c-1PD f -PI) controller designed for effective speed control of brushless DC (BLDC) motors is introduced in [18], it demonstrates superior performance compared to traditional

controllers through numerical simulations and experiment results.

The objective of this work attempts to present a comparative analysis of different PI-based control techniques for speed regulation of a squirrel-cage induction motor. The performance of each controller is examined under varied load conditions and reference speed profiles based on comprehensive simulations using MATLAB/Simulink. The goal is to discover the most effective control strategy for ensuring robustness, adaptability and fast response.

The main contributions of this research are summarized as follows:

1. The proposition of four modified speed regulators based on conventional PI.
2. The development of these enhanced speed regulators.
3. Improve the robustness of these speed regulators.
4. Development of a controller more performant than the conventional PI regulators with a minimum cost.

The remainder of the manuscript is organized as follows: in Section 2, the mathematical model of the studied induction motor is presented. The control strategy of the five proposed controllers is described in Section 3. Primary part of Section 4 shows the numerical simulation results of the controllers PI, IP, HPI, PI Anti-windup and VGPI. A performance evaluation of each controller is also evoked. The second part of Section 4 is focused on the quantitative performance comparison of the controllers. Finally, a conclusion is presented in Section 5.

2. MATHEMATICAL MODELING OF THE INDUCTION MOTOR

The dynamic behaviour of the induction motor is modelled using the standard d-q axis equations in the synchronous reference frame [19]. The mathematical model includes stator and rotor voltage equations, flux linkages and electromagnetic torque expressions. The model assumes balanced three-phase inputs, neglects magnetic saturation and core losses for simplicity. The extended nonlinear state-space model (with the load torque introduced as a state variable) of the induction machine in the generalized rotating d-q reference frame is:

$$\frac{d}{dt}\begin{bmatrix} i_{sd} \\ i_{sq} \\ \emptyset_{rd} \\ \emptyset_{rq} \\ \Omega \\ T_L \end{bmatrix} = \begin{bmatrix} -\gamma i_{sd} + \omega_s i_{sq} + ba\emptyset_{rd} + bp\Omega\emptyset_{rq} \\ -\omega_s i_{sd} - \gamma i_{sq} - bp\Omega\emptyset_{rd} + ba\emptyset_{rq} \\ aL_m i_{sd} - a\emptyset_{rd} + (\omega_s - p\Omega)\emptyset_{rq} \\ aL_m i_{sq} - (\omega_s - p\Omega)\emptyset_{rd} - a\emptyset_{rq} \\ m\left(\emptyset_{rd} i_{sq} - \emptyset_{rq} i_{sd}\right) - c\Omega - \frac{1}{J}T_L \\ 0 \end{bmatrix} + \begin{bmatrix} m_1 & 0 \\ 0 & m_1 \\ 0 & 0 \\ 0 & 0 \\ 0 & 0 \\ 0 & 0 \end{bmatrix} \begin{bmatrix} u_{sd} \\ u_{sq} \end{bmatrix} \quad (1)$$

where: i_{sd}, i_{sq} - Respectively, the direct and quadrature components of the stator current (A), u_{sd}, u_{sq}, - respectively, the direct and quadrature components of the stator voltage (V), $\emptyset_{rd}, \emptyset_{rq}$ - respectively, the direct and quadrature components of the rotor, $\emptyset_r$ - a rotor flux (wb), T_L - the load torque (Nm), $\omega_r, \omega_s, \omega_g$ - are respectively, the electrical angular velocities of the rotor, the stator, the slip of the motor (rad/s), Ω - the mechanical angular velocity of the motor (rad/s).

( )* - indicates the reference quantities of the control inputs.

The parameters $a, b, c, \gamma, \sigma, m, m_1$ and are defined as follows:

$$\sigma = 1 - \frac{L_m^2}{L_s L_r}, a = \frac{R_r}{L_r}, b = \frac{L_m}{\sigma L_s L_r}, c = \frac{f_c}{J}$$

$$\gamma = \frac{L_r^2 R_s + L_m^2 R_r}{\sigma L_s L_r^2}, m = \frac{pL_m}{JL_r}, m_1 = \frac{1}{\sigma L_s}$$

If the following choice is adopted:

$$x^T = [\emptyset_{rd} \quad \emptyset_{rq} \quad i_{sd} \quad i_{sq}]$$

$$y^T = [T_e \quad \emptyset_r^2]$$

then the state-space representation becomes:

$$\frac{d}{dt}\begin{bmatrix} \emptyset_{(d,q)}^r \\ \sigma i_{(d,q)}^s \end{bmatrix} = \begin{bmatrix} -\frac{1}{T_r} & (\omega_s - \omega) & \frac{L_r}{T_r} & 0 \\ -(\omega_s - \omega) & -\frac{1}{T_r} & 0 & \frac{L_r}{T_r} \\ \frac{L_m}{L_s L_r T_r} & \frac{L_m \omega}{L_s L_r} & -\frac{R_r}{L_s} & \sigma\omega_s \\ -\frac{L_m \omega}{L_s L_r} & \frac{L_m}{L_s L_r T_r} & -\sigma\omega_s & -\frac{R_r}{L_s} \end{bmatrix} \begin{bmatrix} \emptyset_{(d,q)}^r \\ i_{(d,q)}^s \end{bmatrix} + \begin{bmatrix} 0 & 0 \\ 0 & 0 \\ \frac{1}{\sigma L_s} & 0 \\ 0 & \frac{1}{\sigma L_s} \end{bmatrix} \begin{bmatrix} u_{sd} \\ u_{sq} \end{bmatrix} \quad (2)$$

$$y = h(x) = \begin{bmatrix} T_e \\ \emptyset_r^2 \end{bmatrix} \quad (3)$$

The vectors: $\frac{d\emptyset_r}{dt}$, and $\sigma\frac{di_s}{dt}$ - represent respectively, the slow and fast modes of the model. $0 < \sigma < 1$

where: R_s, R_r - respectively, the rotor and the stator resistances (Ω), L_s, L_r, L_m - respectively, the cyclic inductances of the stator, the rotor, and the mutual inductance (H), $p,\ J, f_c$ - respectively, the number of pole pairs, the moment of inertia, and the viscosity coefficient, T_r, σ - are respectively, the rotor time constant, and the Blondel dispersion coefficient, T_e - represent the electromagnetic torque (Nm).

3. CONTROL STRATEGY

The control system is based on indirect field-oriented control [20], which aligns the rotor flux along the d-axis and decouples the torque and flux control (Fig. 1).

The outer speed control loop uses the PI, HPI, VGPI, or Anti-Windup PI controller to generate the reference current for the inner current loops.

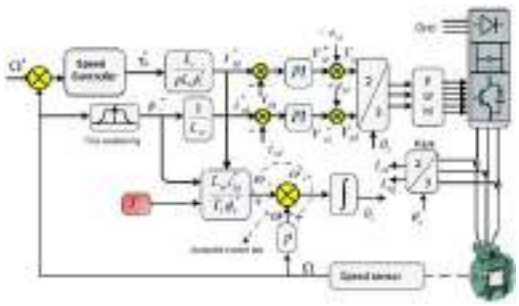

Fig. 1. Global block diagram of Indirect Field-Oriented Control

3.1. Speed control

To improve the dynamic performance of speed regulation in an Indirect Field-Oriented Control (IFOC) scheme, alternative controllers such as the Integral-Proportional (IP) [21], Hysterisis PI [16], PI Anti-windup [23-24], and Variable Gain PI (VGPI) [25] controllers are implemented instead of the conventional Proportional-Integral controller.

3.1.1. PI controller (Proportional-integral controller)

To improve the dynamic performance of speed regulation in an Indirect Field-Oriented Control (IFOC) scheme, alternative controllers such as the Integral-Proportional (IP) [21], Hysteresis PI [16], PI Anti-windup [23-24], and Variable Gain PI (VGPI) [25] controllers are implemented instead of the conventional Proportional-Integral controller.

The PI controller is a classical control strategy that combines proportional and integral actions to minimize the error between a system's desired and actual outputs.

$$u(t) = k_p e(t) + k_i \int_0^t e(\tau)d\tau \tag{4}$$

where:
$u(t)$ - controller output (reference torque or speed
$e(t)$ - error signal
k_p, k_i - respectively, proportional gain and integral gain

To design the PI controller, the dynamic induction motor model is considered under the regulated rotor flux assumption. Given that the current control loop (electrical dynamics) responds much faster than the speed control loop (mechanical dynamics). The stator current components i_{sd}, i_{sq} are assumed to follow their reference values instantaneously. This time-scale separation allows for a simplified controller design focused on mechanical dynamics. The speed controller block diagram is presented in (Fig. 2):

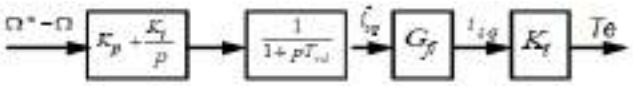

Fig. 2. Block diagram of the speed controller

where: k_p, k_i - are PI controller gains, T_{vd} - Computation time delay, G_{fi} - Current loop transfer function, $K_t = \frac{3}{2} p \frac{L_m}{L_r} \emptyset_r^*$ - Motor torque constant, Ω - the mechanical angular velocity (rad/s), ( )* - indicates the reference quantities or the control inputs.

In order to simplify the computation of the parameters related to this type of controller, the block diagram shown in (Fig. 2) is assumed to be reducible to a classical PI controller. To this end, the delay T_{vd} as well as the current loop dynamics are neglected with respect to the speed dynamics.

The resulting expression is then given by:

$$\Omega = \frac{k_p p + K_i}{JP^2 + (k_p + f_c)p + k_i} \Omega_{ref} - \frac{p}{JP^2 + (k_p + f_c)p + k_i} T_L \tag{5}$$

The transfer function derived from Eq. (5) can be expressed as a second-order system of the form:

$$F(p) = \frac{1}{1 + \frac{2\varepsilon}{w_n} p + \frac{p^2}{w_n^2}} \tag{6}$$

where, ε - denotes the damping ratio, ωn - represents the undamped natural frequency.

The following identities can be established:

$$\begin{cases} \frac{J}{k_i} = \frac{1}{w_n^2} \\ \frac{2\varepsilon}{w_n} = \frac{k_p + f_c}{k_i} \end{cases} \tag{7}$$

It is worth recalling the expressions for the system's overshoot, $D\% = 100e^{-\frac{\pi\xi}{\sqrt{1-\xi^2}}}$ and 5% settling time $t_{5\%} \approx \frac{3}{\xi\omega_n}$

3.1.2. IP controller (Integral-proportional controller)

The block diagram of an IP controller is shown in Fig.3. This type of controller applies a proportional action to the measured output and an integral action to the error, ensuring the elimination of the steady-state error.

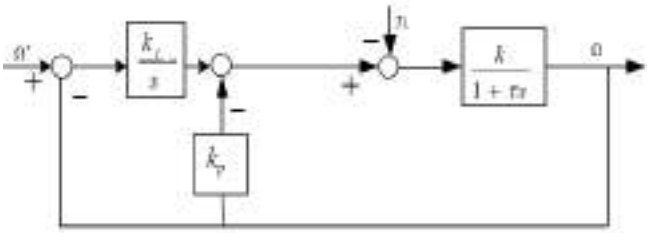

Fig. 3. Block Diagram of an Integral-Proportional (IP) Speed Controller

where: $k = \frac{1}{f_c}, \tau = \frac{J}{f_c}$ - the mechanical time constant, f_c - viscous friction coefficient.

Accordingly, the following identities can be established:

$$\Omega = \frac{\frac{kk_i}{\tau}}{s^2 + s\frac{1+kk_p}{\tau} + \frac{kk_i}{\tau}} \Omega^* - \frac{s\frac{k}{\tau}}{s^2 + s\frac{1+kk_p}{\tau} + \frac{kk_i}{\tau}} T_L \tag{8}$$

$$\begin{cases} k_p = \frac{2\xi\omega_n\tau - 1}{k} \\ k_i = \frac{\omega_n^2 \tau}{k} \end{cases} \tag{9}$$

3.1.3. HPI controller (Hysteresis PI controller)

The HPI controller is an advanced form of the PI controller that includes a dynamic adaptation of the gains for better performance in terms of robustness and system stability [26].

$$u(t) = k_p e(t) + k_i \int_0^t e(\tau)d\tau + f(\theta) \tag{10}$$

where: $f(\theta)$ - A dynamic gain adaptation function dependent on the hysteresis threshold h, h - defines the hysteresis band on the speed error $(-\mathrm{e(t)} \leq \mathrm{h} \leq +\mathrm{e(t)})$.

3.1.4. PI anti-windup (High-performance PI controller)

The actuator is saturated when the anti-windup PI controller is designed to prevent integrator windup by correcting the integral term [27]. The control law is modified by adding feedback correction

proportional to the difference between the saturated and unsaturated control signals. (Fig. 4).

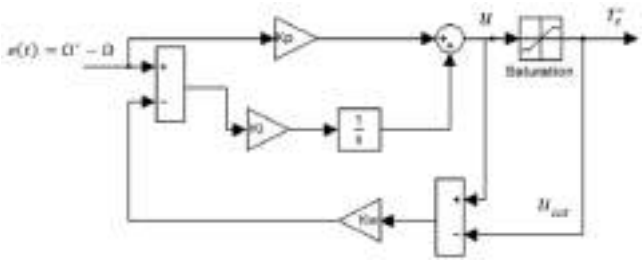

Fig. 4. Block Diagram of a PI Antiwindup Speed Controller

The control law is given as below:

$$u(t) = k_p e + \frac{1}{T_i}\int_0^t (\dot{e} - (u - u_{sat})k_w)dt \quad (11)$$

where: $u_{sat} = sat(u) = \begin{cases} u_{min} & if \quad u < u_{min} \\ u & if \quad u_{min} \le u < u_{max} \\ u_{max} & if \quad u > u_{max} \end{cases}$

k_w - is the anti-windup gain, $u_{sat}(t)$ - is the saturated control signal, $u(t)$ - is the pre-saturation signal

When saturation occurs, the feedback mechanism modifies the integral action to bring the error toward zero while keeping the controller output at the saturation boundary.

3.1.5. VGPI controller (Variable-gain PI controller)

The VGPI controller adjusts the controller gains based on the system's state or operating conditions to improve performance in varying environments [28]. This is typically used in time-varying parameter systems.

$$u(t) = k_p e(t) + k_i \int_0^t e(\tau)d\tau \quad (12)$$

$$k_p = \begin{cases} (k_{pf} - k_{if})\left(\frac{t}{t_s}\right)^n + k_{pi} & si \quad t < t_s \\ k_{pf} & si \quad t \ge t_s \end{cases}$$
$$k_i = \begin{cases} k_{if}\left(\frac{t}{t_s}\right)^n & si \quad t < t_s^n \\ k_{if} & si \quad t \ge t_s \end{cases} \quad (13)$$

where: $e(t)$ - is the error signal, and $\mathrm{k_p}, \mathrm{k_i}$ - are respectively, time-varying proportional gain and time-varying integral gain

k_{pi} , k_{pf} - Are respectively the initial and final values of the proportional gain, k_{if} - is the final value of the integral gain, while the initial value of the integral gain is considered zero to help eliminate overshoot, t_s - is the saturation time, n - the degree of the transient response function, defined as the degree of the variable gain controller.

3.2. Computational burden analysis

From a computational point of view, the classical PI and IP controllers present the lowest complexity due to their simple linear structure and minimal arithmetic operations, Eqs. (6-9).

The anti-windup PI controller introduces a slight additional computational burden due to the integrator saturation mechanism, which requires a few extra operations per cycle to handle windup correction. In contrast, the HPI and VGPI controllers require higher computational effort due to nonlinear gain adaptation and time-varying parameters.

In contrast, the HPI controller demands higher computational effort because of its nonlinear hysteresis logic and gain adaptation rules. The VGPI controller requires the most significant overhead, as it involves real-time calculation of time-varying gains based on the scheduling law given in Eq. (13).

Given the relatively low number of operations involved, all controllers are considered algorithmically feasible for real-time implementation within typical motor-control sampling periods on common digital platforms such as DSPs or microcontrollers

3.3. Controller parameter values

Using the motor parameters from Tab. 2, the base proportional and integral gains k_p & k_i are calculated from Eq. (7).

The values of the controller gains used in the simulation were calculated mathematically and subsequently fine-tuned using the trial-and-error method.

All speed controller parameters used in the simulations are summarized in Tab. 1.

Tab. 1. Controller parameters

Controller	Parameter	Value	Remark
Classical PI	k_{pv}	49.6	Proportional gain
	k_{iv}	3.1	Integral gain
IP	k_{pv}	49.6	Same as PI, structure differs
	k_{iv}	3.1	Same as PI
HPI	k_{pv}	49.6	Base proportional gain
	k_{iv}	3.1	Base integral gain
	h	0.01	Hysteresis band
PI Anti-windup	k_{pv}	49.6	Proportional gain
	k_{iv}	3.1	Integral gain
	k_{aw}	0.5	Anti-windup correction gain
VGPI	$k_{p,i}$	10	Initial proportional gain *(allow the elimination of speed overshoot)*
	$k_{p,f}$	60	Final proportional gain *(allow the elimination of speed overshoot)*
	$k_{i,i}$	0	Initial integral gain
	$k_{i,f}$	100	Final integral gain (*rapid rejection of load disturbances)*
	t_s	1	Transition time ($t_s \le 2s$)
	n	3	Transition order

4. SIMULATION RESULTS

The numerical simulations are carried out in MATLAB/Simulink using the same motor parameters and load conditions. The test scenarios include speed tracking performance for step and ramp

reference changes, load disturbance rejection, and sensitivity to parameter motor variations.

The results are compared in terms of rising time and settling time, overshoot and steady-state error and robustness.

The induction motor parameters are shown in Tab 2.

Tab. 1. Table of the induction motor parameters

R_s	4.850Ω	P_n	1,5kW	f_c	0.00114(Nms/rad)
R_r	3.805Ω	I_n	6.5A	p	2
L_s	0.274H	V_n	220V	f_n	50Hz
L_r	0.274H	ω_n	149rad/s		
L_m	0.258H	J_n	0.031kg/m^2		

4.1. Classical profile

In this test scenario, the reference speed is defined as a smooth step reaching 100 rad/s. The reference flux is maintained at 1Wb throughout the simulation.

A constant load torque of $T_L = 10Nm$, is applied between t=1s and t=2s.

This profile serves as a benchmark case evaluation for the nominal behavior and baseline performance of the proposed control strategies under standard operating conditions.

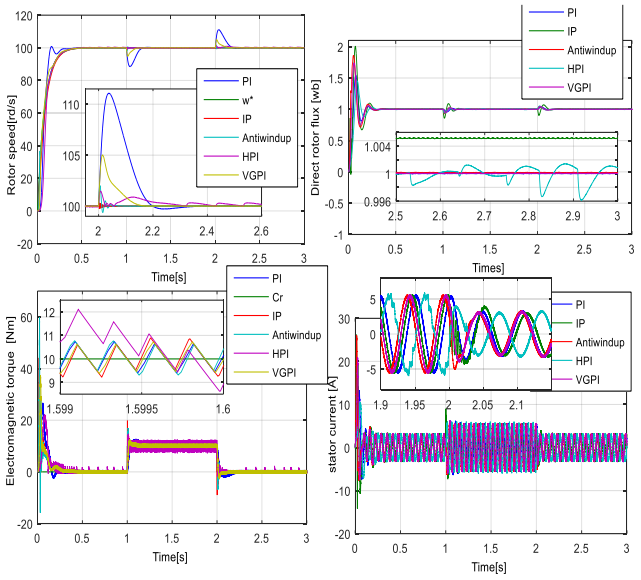

Fig. 5. Performance of the speed control strategies under standard operating (Classical profile)

According to the simulation results shown in (Fig. 5), the following observations can be done:

The PI and VGPI controllers exhibit the highest overshoots and demonstrate weaker disturbance rejection capabilities. The simulation results of the stator three-phase currents show that no overshoot is observed, confirming the effectiveness of current limitation.

Under load disturbance, the HPI (Hysteresis PI) controller appears to deliver superior performance. With an appropriate chosen parameter value, it effectively dampens speed oscillations.

The value h=0.01 is chosen for simulation to demonstrate precise speed regulation under ideal conditions. In practice, h can be adjusted based on sensor resolution and noise tolerance.

The speed response illustrated in (Fig. 5), demonstrates that following the application of a load torque of 10 Nm at t = 0.5s, the actual speed tracks the reference speed. However, notable transient phenomena are observed, characterized by pronounced overshoot and disturbance rejection effects.

The PI Anti-windup and IP controllers show improved performance in the presence of load disturbances.

4.2. Critical operating conditions

4.2.1. Speed reversal profile

A reversal in the direction of rotation is imposed between *t*=1s and *t*=2s. The reference flux, $\emptyset^* = 1wb$. A constant load torque of 10 Nm is applied starting at *t*=0.5s (Fig.6).

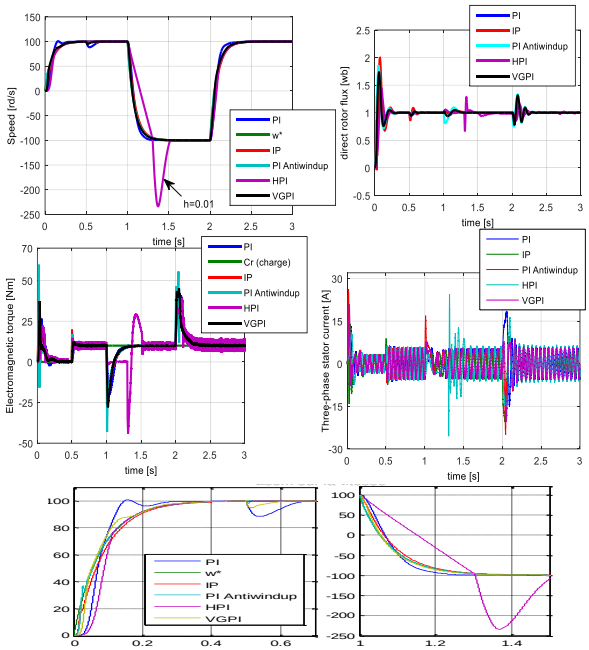

Fig. 6. Comparison of different speed controllers under a speed reversal profile

The conventional PI controller exhibits the weakest disturbance rejection capability and the highest overshoot among all the tested strategies. Similarly, the VGPI controller demonstrates limited effectiveness in disturbance rejection. Although the HPI controller fails to maintain accurate speed tracking during deceleration phases. It achieves superior performance in rejecting external disturbances.

In contrast, both of the IP controller and the anti-windup PI controller deliver the best overall performance, excelling in both speed tracking and disturbance rejection.

4.2.2. Impact of parametric variations on IFOC performance

This scenario evaluates the robustness of the controllers under parametric uncertainties. The rotor resistance R_r varies by 50% and +100% of its nominal value $R_{rn} = 3.805\Omega$, while the moment of inertia J is altered by -50%,100% and 400%.

The reference speed is maintained at 100 rad/s, with a constant load torque of 10 Nm applied between t=1s and t=2s.

DOI: 10.65731/ama/2026-0023

According to the numerical simulation results for the critical profiles, (Figs.7 - 11).

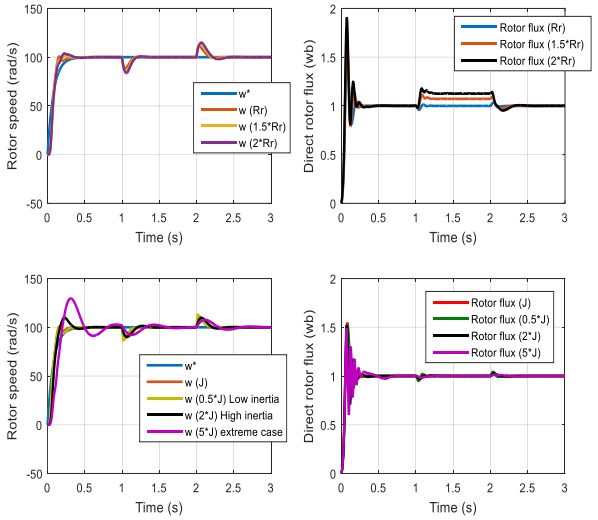

Fig. 7. Robustness of PI speed controller against parametric uncertainties

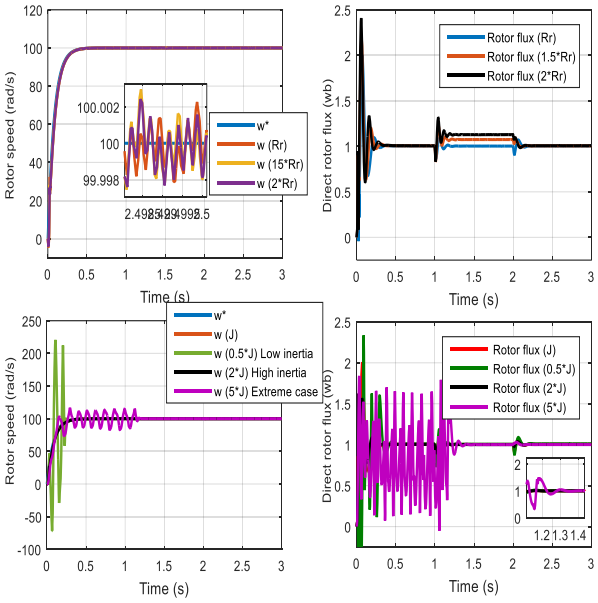

Fig. 8. Robustness of IP speed controller against parametric uncertainties

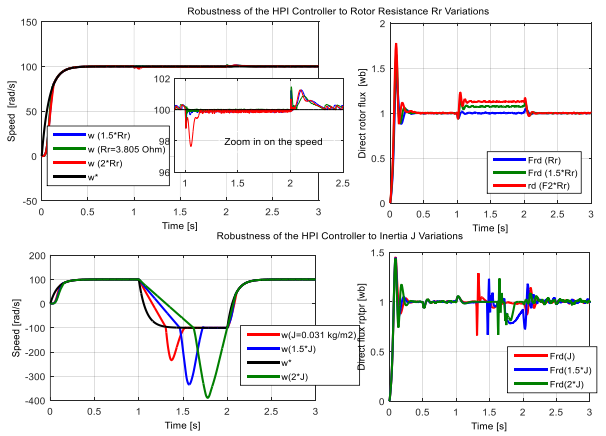

Fig. 9. Robustness of HPI speed controller against parametric uncertainties

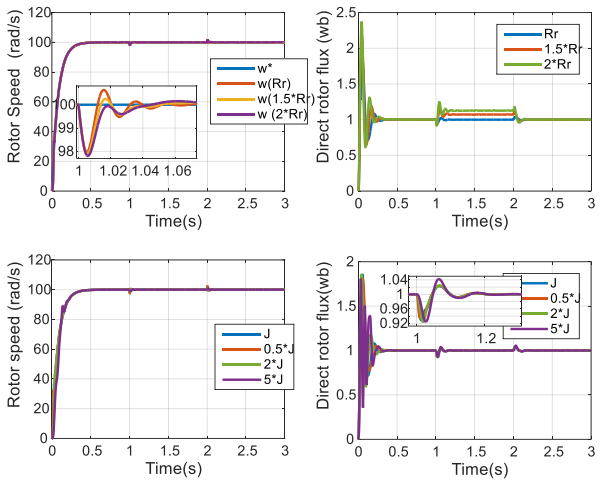

Fig. 10. Robustness of PI-Antiwindup speed controller against parametric uncertainties

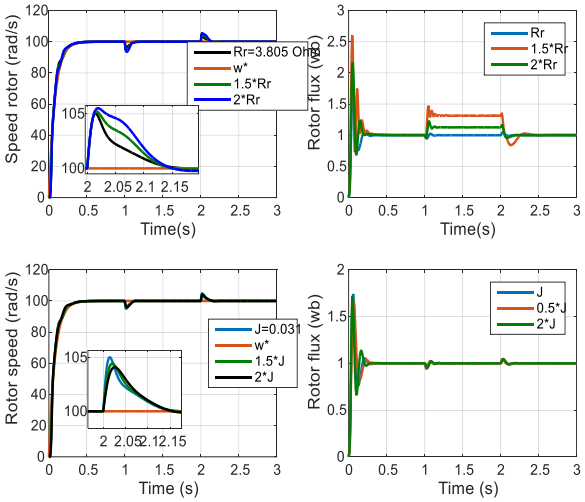

Fig. 11. Robustness of variable gain PI speed controller against parametric uncertainties

The following observations can be made: while each controller exhibited satisfactory performance in both speed tracking and disturbance rejection, none succeeded in achieving robust decoupling against variations in the most influential parameter within an IFOC strategy, specifically the rotor resistance

The IP, VGPI, and PI Anti-windup controllers exhibit satisfactory performance under various conditions, including load disturbances (Fig.5), speed-tracking (Fig.6), and even in the presence of machine parameter variations (Figs. 7- 11).

Table 3 summarizes the Mean Square Error (MSE), Integral Absolute Error (IAE), and Integral Squared Error (ISE) computed over the same evaluation interval for all controllers.

The metrics performance summary for the various speed controllers, highlighting key aspects such as disturbance rejection, speed tracking accuracy, and overshoot behavior are presented in Tab 4.

The quantitative performance indices (Tab. 3) confirm the qualitative (Tab. 4) observations. The VGPI controller exhibits the lowest MSE, IAE, and ISE values, indicating superior reference tracking accuracy and disturbance rejection. The PI anti-windup and HPI controllers also show improved performance compared to the classical PI and IP controllers, particularly under load disturbances and

parametric variations.

Tab. 3. Quantitative performance comparison of speed controllers

Controller	MSE (rad^2/s^2)	IAE (rad)	ISE (rad^2/s)	Computational burden
Classical PI	0.052	0.559	0.156	Low
IP	0.031	0.431	0.093	Low
HPI	0.021	0.355	0.063	Medium
PI-Anti windup	0.014	0.290	0.042	Medium
VGPI	0.008	0.219	0.024	High

Tab. 4. Qualitative performance metrics of speed controllers.

Controller	Overshoot	Setting time	Steady-state error	Robustness
Classical PI	High	Moderate	Low	Weak
IP	Low	Moderate	Very low	Moderate
HPI	Low	Fast	Very low	Good
PI-Anti windup	Moderate	Fast	Low	Moderate
VGPI	Very Low	Very Fast	Zero	Excellent

5. CONCLUSION

This study represents a comprehensive comparative analysis of several PI-based controllers namely the classical PI, Integral-Proportional (IP), Hyperbolic PI (HPI), PI with anti-windup compensation, and Variable Gain PI (VGPI) for the speed regulation of an induction motor under field-oriented control. The objective is to assess their dynamic robustness and performance in the presence of nonlinearities and parametric uncertainties.

The classical PI controller, despite its widespread use and simplicity, shows limitations in terms of overshoot, settling time and robustness against parameter variations. The IP controller demonstrated improved damping characteristics and reduced overshoot but remained moderately sensitive to system uncertainties. The HPI controller, by introducing nonlinear characteristics through hyperbolic functions, achieved a superior balance between fast response and robustness, particularly under transient conditions.

The anti-windup PI controller significantly mitigated the adverse actuator saturation effects, leading to improved dynamic performance. Finally, the VGPI controller, which adapts its gains in real-time based on system behaviour, consistently outperformed the others across all metrics evaluation, particularly in robustness, tracking precision and disturbance rejection. The results of our work will serve as a reference for comparison with other types of controllers (scheduling controller, sliding controller, fuzzy controller, etc.).

REFERENCES

1. Talaoubrid A, Aitgougam Y, Dermouche R, Boucherit M. S. Experimental comparison of the performance of PI and IP controllers for a field-oriented controlled permanent magnet synchronous motor drive. International Journal of Dynamics and Control. 2024;12:2918–2928. https://doi.org/10.1007/s40435-024-01395-7
2. Wang F, Zhang Z, Mei X, Rodríguez J, Kennel, R. Advanced Control Strategies of Induction Machine: Field Oriented Control, Direct Torque Control and Model Predictive Control. *Energies*. 2018; 11(1): 120. https://doi.org/10.3390/en11010120
3. Acikgoz H, Kececioglu OF, Gani A, Sekkeli M. Speed Control of Direct Torque Controlled Induction Motor By using PI, Anti-Windup PI And Fuzzy Logic Controller. International Journal of Intelligent Systems and Applications in Engineering. 2016; 4(3):105–110. https://doi.org/10.18201/ijisae.26422
4. Gao Y, Zhang Y, Li X, Wang H, Liu J. A novel exponential-type anti-windup method applied to the power converter in marine electrical propeller system. IET Power Electronics. 2022; 15(2). https://doi.org/10.1049/pel2.12250
5. Chiah C, Tan KK, Lee TH. Study of anti-windup PI controllers with different coupling–decoupling tuning gains in motor speed. Asian Journal of Control. 2022;24(1). https://doi.org/10.1002/asjc.2669
6. Jain JK, Ghosh S, Maity S. Concurrent PI Controller Design for Indirect Vector Controlled Induction Motor. *Asian Journal of Control*. 2020; 22(1):130–142. https://doi.org/10.1002/asjc.1911
7. Chikouche TM, Mezouar A, Terras T, Hadjeri S. Variable Gain PI Controller Design For Speed Control of a Doubly Fed Induction Motor Using State-Space Nonlinear Approach. *Engineering, Technology& Applied Science Research*. 2013;3(3): 433–439. https://doi.org/10.48084/etasr.305
8. Hoo CL, Haris SM, Chung ECY, Mohamed NAN. New Integral Antiwindup Scheme for PI Motor Speed Control. Asian Journal of Control. 2015;17(6): 2115–2132. https://doi.org/10.1002/asjc.1144
9. Aichi, B, Kendouci K. A Novel Switching Control for Induction Motors Using a Robust Hybrid Controller that Combines Sliding Mode with PI Anti-Windup.Periodica Polytechnica Electrical Engineering and Computer *Science*. 2020; 64(4): 392–405. https://doi.org/10.3311/PPee.15661
10. Meng LQ, Li M J. A New Anti-Windup PI Controller for Direct Torque Control System. Indonesian Journal of Electrical Engineering and Computer Science. 2013; 12(7): 5268–5274. https://doi.org/10.11591/ijeecs.v12.i7.pp5268-5274
11. Oliveira CMR, Aguiar ML, Monteiro JRBA, Pomilio JA. Vector Control of Induction Motor Using an Integral Sliding Mode Controller with Anti-windup. Journal of Control, Automation and Electrical Systems. 2016; 27:169–178. https://doi.org/10.1007/s40313-016-0228-4
12. Ouboubker L, Lamterkati J, Khafallah M, El Afia A. Real time implementation of anti-windup PI controller for speed control of induction machine based on DTC strategy. *International Journal of Power Electronics and Drive Systems*. 2021;12(3):1358–1368. http://doi.org/10.11591/ijpeds.v12.i3.pp1358-1368
13. El Daoudi S, Lazrak L, El Ouanjli N, et al. Applying sliding mode technique for the nonlinear DTC-SPWM control strategy of sensorless squirrel cage asynchronous motor. Int. J. Dynam. Control. 2021; 9: 1633–1644. https://doi.org/10.1007/s40435-021-00758-8
14. El Daoudi S, Lazrak L, El Ouanjli N, et al. Improved DTC-SPWM strategy of induction motor by using five-level POD-PWM inverter and MRASSF estimator. Int. J. Dynam. Control. 2021;9:448–462. https://doi.org/10.1007/s40435-020-00667-2
15. El Ouanjli N, Mahfoud S, Saad Al-Sumaiti A, El Daoudi S, Derouich A, El Mahfoud M, Mossa M A. Improved twelve sectors DTC strategy of induction motor drive using Backstepping speed controller and P-MRAS stator resistance identification-design and validation. Alexandria Engineering Journal. 2023;80:358-371. https://doi.org/10.1016/j.aej.2023.08.077
16. Çelik E, Bal G, Öztürk N, et al. Improving speed control characteristics of PMDC motor drives using nonlinear PI control. Neural Comput& Applic. 2024; 36: 9113–9124. https://doi.org/10.1007/s00521-024-09568-3
17. Çelik E, Öztürk N. First application of symbiotic organisms search algorithm to off-line optimization of PI parameters for DSP-based DC motor drives. Neural Comput & Applic. 2018, 30, 1689–1699. https://doi.org/10.1007/s00521-017-3256-5
18. Çelik E, Karayel M. Effective speed control of brushless DC motor using cascade 1PDf-PI controller tuned by snake optimizer. Neural Comput & Applic. 2024; 36: 7439–7454. https://doi.org/10.1007/s00521-024-09470-y

19. Arindam M, Prasanta S, Aliprio H. A unified approach for PI controller design in delta domain for indirect field-oriented control of induction motor drive. Journal of Engineering Research. 2020; 8(3): 1–10. https://doi.org/10.36909/jer.v8i3.7872Kuwait Journals
20. Md Hairul Nizam T, Zulkifilie I, Nasrudin A R, Abu Hasim A S. Comparison Analysis of Indirect FOC Induction Motor Drive using PI, Anti-Windup and Pre Filter Schemes. International Journal of Power Electronics and Drive Systems. 2014; 4(4): 6250.
21. Khelifa Khelifi O. Anti-windup GPC speed controller for induction machine based on Youla parametrization. Journal of Electrical Engineering. 2022;73(1):50–56.https://doi.org/10.2478/jee-2022-0007
22. Boucherit MS, Dahal K. P. Design and performance analysis of anti-windup PI controllers for the speed control of induction motors. Journal of Electrical Engineering&Technology. 2023;18(4):1250-1261. https://doi.org/10.1007/s42835-023-01477-9
23. Liu X, Zhang W. A comparative study of anti-windup PI controllers for speed regulation of permanent magnet synchronous motors. Journal of Electrical Engineering and Technology. 2021;16(3): 1567-1579. https://doi.org/10.1007/s42835-021-01322-0
24. Rezaei M, Khusainov R. New anti-windup method for the control of synchronous motor drive systems. International Journal of Electrical Power & Energy Systems. 2019; 105: 253-263. https://doi.org/10.1016/j.ijepes.2018.08.012
25. Nouri M, Farahani, M. Anti-windup control for induction motor with field-oriented control: A case study. Journal of Control Engineering and Technology. 2020; 6(1): 29-39. https://doi.org/10.1016/j.jcet.2019.12.001
26. Sarwar A, Ali S. A review on PI, anti-windup PI, and fuzzy logic controllers for induction motor drives. International Journal of Electrical and Computer Engineering. 2022; 12(5): 3503–3511. https://doi.org/10.11591/ijece.v12i5.2823
27. Ebrahimi M, Ali M. Development of an anti-windup scheme for PI controllers used in induction motor drives. Journal of Electrical Engineering and Technology. 2017;12(1):133–141. https://doi.org/10.1007/s42835-017-0010-2
28. Sefidgaran MH, Rahim NA. Hybrid control of induction motor using anti-windup PI and sliding mode controller. International Journal of Control, Automation and Systems. 2019;17(2):353–362. https://doi.org/10.1007/s12555-018-0156-2

Yesma Bendaha: https://orcid.org/0000-0002-1347-856X

Kadda Boumediene: https://orcid.org/0000-0002-5569-3022

Bachir Daaou: https://orcid.org/0000-0002-0939-9164